Energy and AI 25 (2026) 100779

Contents lists available at ScienceDirect

Energy and AI

journal homepage: www.elsevier.com/locate/egyai

Review

Satellite solar radiation forecasting by next-frame prediction — Advances and future opportunities

Angela Meyer *

Department of Geoscience and Remote Sensing, Delft University of Technology, 2628 CN Delft, Netherlands
School of Engineering and Computer Science, Bern University of Applied Sciences, 2501 Biel, Switzerland

ARTICLE INFO

Keywords:
Solar radiation
Forecasting
Solar forecast models
Satellite-based solar forecasts
Deep learning
Surface solar irradiance
Photovoltaics

ABSTRACT

Solar radiation forecasting is essential for operating energy systems with high shares of photovoltaic power generation as solar radiation can fluctuate rapidly with cloud cover and atmospheric conditions. Accurate solar forecasts help utilities and grid operators schedule reserves, balance supply and demand, and reduce reliance on fossil backup. Skilful solar forecasts also support energy market operations, battery control, and congestion management by predicting when and where solar generation will increase or drop. Classic weather prediction models struggle with long forecast latency times, timely assimilation of the latest satellite observations, spatial resolution, and low forecast update frequencies. Satellite-based solar forecast models can outperform classic forecast models for lead times of up to several hours. We review spatiotemporal solar forecast models that leverage satellite observations and machine learning for accurate solar intraday forecasts based on next-frame prediction. We discuss recent progress in this field, opportunities, challenges, and future research directions.

1. Introduction

Solar energy plays a central role in low-carbon energy systems as an abundant, emission-free power source with competitive levelised cost of energy. Solar photovoltaics constitutes a growing share of the electricity supply in many countries [1]. However, surface solar radiation fluctuates strongly in space and time mainly due to the variability of clouds and atmospheric aerosols, making it challenging to forecast the associated radiative effects at the Earth's surface. This volatility poses operational challenges for balancing electricity supply and demand, scheduling reserves, and integrating solar generation in electricity markets [2]. Grid operators require accurate short-term forecasts to maintain grid stability as the integrated solar power fluctuates. At energy markets, forecasts influence prices and determine intraday strategies and dispatch schedules. Inaccurate forecasts can cause supply and demand imbalance and result in higher operating costs. System operators must procure enough flexible capacity to compensate for unexpected deviations in solar power yield. Improving the accuracy of SSI forecasts can reduce reserve requirements and decrease reliance on fossil backup generation. Accurate forecasts of surface solar irradiance (SSI) are therefore essential for ensuring the economic and reliable operation of solar-rich energy systems [3,4].

Surface solar irradiance refers to the incoming electromagnetic irradiance originating from the sun that is incident on a horizontally oriented plane at the Earth's surface per unit area per unit time, integrated across the solar spectral range of 0.3–3 μm. It includes radiation arriving from all directions of the upper hemisphere above the plane of incidence and comprises both the direct solar beam and diffuse radiation scattered by atmospheric constituents. SSI represents a surface power density ($W\,m^{-2}$), equivalently expressed as an energy flux ($J\,s^{-1}\,m^{-2}$), describing the amount of solar energy received per unit area per unit time. Depending on the discipline, SSI is also known as global horizontal irradiance, shortwave downward flux, and surface downwelling shortwave radiation [5,6]. SSI is commonly measured using broadband radiometers known as pyranometers, which typically employ thermopile sensors that absorb SSI, generating a temperature gradient and a corresponding voltage signal from which SSI is inferred.

SSI results from the radiative effect that clouds, atmospheric aerosols and radiatively active gases such as water vapour, carbon dioxide and ozone exert at the Earth's surface. Among them, clouds are the most important factor influencing SSI through their optical properties, motion, and life cycle. Cloud-related variability in SSI is caused by processes across a wide range of spatial and temporal scales, encompassing synoptic-scale weather systems, local to mesoscale cloud organisation, and cloud microphysics [7]. SSI tends to be challenging to predict as it depends critically on the properties and evolution of clouds, including their optical thickness, phase, and structure, all of which can evolve rapidly. Small cloud features can change SSI on time scales of seconds to minutes whereas larger cloud structures introduce

* Correspondence to: Department of Geoscience and Remote Sensing, Delft University of Technology, 2628 CN Delft, Netherlands.
E-mail address: angela.meyer@tudelft.nl.

https://doi.org/10.1016/j.egyai.2026.100779
Received 1 February 2026; Received in revised form 21 April 2026; Accepted 19 May 2026
Available online 25 May 2026

less rapid, longer-term variability. The temporal evolution of cloud cover is scale-dependent, and SSI forecast skill improves when this scale dependence is represented in the forecast model [8]. Classic weather prediction models are typically operated at horizontal resolutions of several kilometers and with hourly or multi-hourly time steps [9,10]. Although processes that cannot be resolved at these scales are parameterised, subgrid-scale clouds and aerosols and their associated radiative effects at the surface remain a major source of forecast uncertainty. In addition, conventional weather prediction models do not forecast in near-real-time but have forecast production times of typically more than five hours from global model initialisation to forecast dissemination [11]. When it comes to intraday SSI forecasting, this combination of coarse resolution and forecast latency places classic weather prediction models at a disadvantage compared to satellite-based SSI forecast models.

Intraday SSI forecasting approaches cover a broad range of methods [12–14]. In addition to conventional weather prediction models, a variety of data-driven SSI forecasting methods have been proposed. Approaches using ground-based observations as input usually rely on pyranometers or sky camera measurements. While such methods can achieve high local accuracy, ground-based observations only represent the conditions in a small area of typically a few square kilometers, which limits their applicability for spatiotemporal forecasting across extended regions [15,16]. Given their wide spatial coverage, SSI fields derived from geostationary satellites are well suited for spatiotemporal SSI forecasting across wide areas and naturally enable simultaneous SSI forecasts for multiple locations. Various satellite-based SSI forecasting approaches have been proposed that rely on statistical or classic machine learning techniques to forecast SSI only at individual sites, e.g., [17–22]. In contrast, this review focuses on satellite-based forecast models that can predict dense SSI fields across large spatial domains, ranging from approximately $1\,\mathrm{km}$ to thousands of kilometres, for lead times of up to a few hours. This review concentrates on methods that formulate SSI forecasting as a next-frame prediction problem by regarding a sequence of satellite images as video frames with the objective to predict subsequent frames. This review excludes methods that mainly rely on ground-based sensors and approaches applying statistical or classic machine learning techniques not inherently adapted for next-frame prediction. This review also excludes studies that forecast only components of SSI, notably direct and diffuse solar irradiance, or cloud-related variables [23,24].

Our paper is structured as follows. Section 2 outlines principles of forecasting SSI from satellite observations. Section 3 reviews existing spatiotemporal SSI forecasting methods that rely on satellites and next-frame prediction with deep learning techniques. Section 4 discusses the emerging field of probabilistic spatiotemporal SSI forecasting methods whereas Section 5 outlines SSI forecast validation methods and operational deployment. Finally, Section 6 discusses opportunities and challenges, and outlines research needs and future directions.

2. Principles of satellite-based SSI forecasting

Satellite-based spatiotemporal forecasts for lead times of up to a few hours rely on geostationary satellites, such as Meteosat, the Geostationary Operational Environmental Satellite (GOES), Fengyun, and Himawari, thanks to their continuous monitoring of the same field of view. These satellites monitor Earth in a dozen or more spectral channels at visible and infrared wavelengths, providing updates at intervals of about 2.5–15 min and spatial resolution on the order of $1\,\mathrm{km}$ at nadir. This enables monitoring of cloud motion and optical properties, cloud top heights, surface temperatures, fog, aerosols, water vapour, ozone and other trace gases.

SSI has been estimated from satellites since the 1970s [25,26]. Heliosat refers to a family of algorithms that retrieve SSI estimates from geostationary satellite observations [27,28]. Heliosat algorithms estimate pixel-level reflectances from satellite-measured radiances, and compute a cloud index from the reflectances that quantifies how SSI is attenuated by clouds. Using a clear-sky model that computes the clear-sky SSI in the absence of clouds at any given location, all-sky SSI is subsequently obtained from cloud attenuation as measured by the cloud index. The clear-sky SSI is estimated from radiative transfer calculations that account for wavelength-dependent scattering and absorption of the incoming light as it propagates through a cloud-free reference atmosphere [29]. Validating and calibrating the estimated SSI with ground-measured SSI is generally needed to obtain reliable estimates of instantaneous SSI fields [30] (see Fig. 1).

The radiative effects of clouds on the ground are driven by cloud advection and evolution. Cloud motion vectors (CMVs) have been computed on clear-sky index and SSI field estimates to forecast SSI [31]. CMVs represent the apparent motion of brightness patterns in image sequences of cloud scenes. Solar irradiance forecasting methods that rely on CMV estimation can outperform classic weather forecast models at lead times of up to several hours [32]. A range of techniques have been proposed for estimating CMVs from geostationary satellite imagery for intraday solar forecasting such as cross-correlation and optical flow methods [17,33–35]. Optical flow techniques estimate the apparent motion of intensity patterns in image sequences assuming that a pixel at location (x, y) moving with horizontal velocity components (u, v) at time t maintains a constant gray-value intensity, $I(x, y, t) = I(x+u\,\delta t,\ y+v\,\delta t,\ t+\delta t)$ [36]. Optical flow has been applied extensively in atmospheric remote sensing for estimating horizontal motion vectors of clouds, precipitation and trace gases. [35] compared five different optical flow methods for computing CMVs and applied them to hourly solar irradiance forecasting. They found that the two best performing techniques were total variation regularisation with an L1 fidelity term (TV-L1) and the hierarchical Lucas-Kanade method [37,38]. CMV-based SSI forecasting approaches often involve cloudiness indices such as the clear-sky index, CSI, which is the ratio of all-sky SSI and clear-sky SSI [8,39]. CSI is a dimensionless proxy of the radiative effect of clouds at the surface. Unlike SSI, CSI can be considered a normalised variable, and the division by clear-sky SSI largely removes diurnal and seasonal SSI variability originating from sun geometry. Modelling CSI allows to largely remove the strong relationship between SSI and the solar zenith angle and thereby separates the cloud radiative effects from the highly predictable clear-sky SSI patterns related to the diurnal and annual cycles. More recently, deep learning-based SSI forecasting models have been shown to outperform optical-flow methods in terms of forecast quality and accuracy [40–45]. These advances motivate the focus of this review on deep learning based forecast models performing next-frame SSI prediction.

3. Spatiotemporal SSI forecasts with deep neural networks

Spatiotemporal SSI forecasting based on geostationary satellites involves predicting the next frame in a sequence of satellite images [46]. Deep network architectures that have been proposed for this task include spatiotemporal recurrent networks, encoder–decoder convolutional neural networks (encoder–decoder CNNs), generative models, and transformer architectures. Spatiotemporal recurrent neural networks (RNNs) such as convolutional long short-term memory networks (ConvLSTMs) and convolutional gated recurrent units (ConvGRU) can simultaneously capture spatial and temporal dependencies by incorporating convolutional structures in recurrent units [47]. Encoder–decoder CNN architectures such as U-Nets [48] compress input images to learn and extract latent-space features, then decompress the downsampled images and map them to future images in the context of SSI nowcasting. To avoid vanishing gradients, skip connections are utilised that allow gradients to propagate more effectively during backpropagation. Encoder–decoder CNNs and spatiotemporal recurrent networks are typically trained on pixel-wise mean squared error (MSE) or mean absolute error (MAE) loss, which can cause spatially blurry SSI forecasts as the model predictions converge to the mean future evolution and

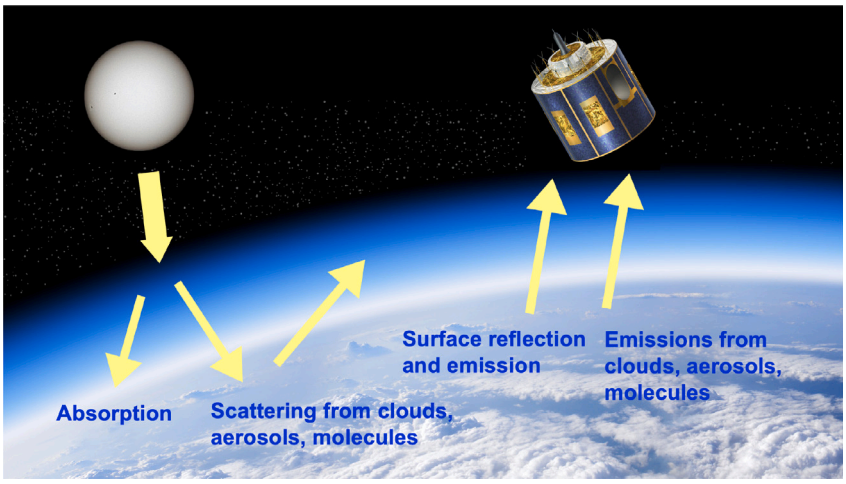

Fig. 1. Visible and infrared radiation reaches the satellite detector after having interacted with atmospheric constituents and the surface by scattering and emission processes.

increasingly lose finer-scale spatial structure. Generative models such as generative adversarial networks (GANs) and diffusion models learn the full distribution of potential future SSI fields rather than deterministically predicting a single mean SSI field at each time step [49, 50]. GANs consist of a generator and a discriminator network. The generator creates new image samples whereas the discriminator seeks to distinguish the generated samples from real images. Generator and discriminator are trained together in an adversarial training process in which the generator learns to create increasingly realistically looking images. Diffusion models estimate probability distributions by training a network to iteratively remove noise that was progressively added to images in a forward process. By repeatedly sampling from the distribution, generative models can predict ensembles of realistically looking sharp future SSI fields. Vision transformers represent images as sequences of patch tokens rather than frames of pixels. Input images are split into patches to be converted into vector embeddings and input to a transformer encoder. Through the self-attention mechanism, transformers have the potential to model long-range spatiotemporal relations and context that may be challenging to capture for convolutional networks which focus more on local short-range relationships. Multiple spatiotemporal SSI forecast models have been proposed to date based on satellite observations and deep networks. We will discuss these models in the following and summarise them in Table 1. For clarity, Table 1 categorises each reviewed SSI forecast model by architecture type and labels it as either deterministic or probabilistic, and as either generative or discriminative, establishing a taxonomy.

3.1. Spatiotemporal recurrent networks

[51] introduce an approach to predict SSI one hour ahead. Their forecast model relies on a ConvLSTM that takes as input SSI derived from the geostationary Korean Communication, Ocean and Meteorological Satellite (COMS) over the Korean Peninsula. The ConvLSTM is shown to outperform a random forest model and a three-layer perceptron that are used as benchmarks. [51] attribute the ConvLSTM's superior performance to the fact that, unlike their benchmark models, the convolutional kernels of the ConvLSTM enable incorporating context from surrounding pixels. [40] present a spatiotemporal SSI forecast model, IrradianceNet, that is based on Meteosat satellite images for forecasts over Europe with lead times of up to four hours. They adopt an autoencoder architecture with ConvLSTM layers that was trained with pixel-wise MSE loss. Input variables include the effective cloud albedo from the Surface Radiation Dataset – Heliosat version 2 (SARAH-2) [52], elevation maps, latitude, longitude and temporal features. Although the model was designed to provide deterministic forecasts, it can, in principle, also be applied for probabilistic forecasts via categorical binning in which the cloud albedo will be assigned to one of 240 different bins, as proposed by [40]. However, this approach to probabilistic forecasting would increase the dimensionality of the output by more than two orders of magnitude which makes the model impractical for multi-step or large-domain forecasts. Following the forecast step, the predicted cloud index is combined with a model of clear-sky SSI to obtain the predicted SSI fields. The model forecasts suffer from increasing blurring with growing forecast lead times due to the MSE loss minimisation. [41] introduce SSI forecasting based on a ConvGRU architecture. Their model has been trained using SSI from the Meteosat Second Generation Cloud Physical Properties (CPP) dataset [53] and predicts 24 future SSI fields at intervals of 15 min, corresponding to a forecast horizon of six hours. The model is benchmarked against an optical flow model and the Weather Research and Forecast (WRF) numerical weather prediction model over the Netherlands. [41] find that their ConvGRU model outperforms these benchmarks in all weather conditions but suffers from blurring of cloud structures with progressing lead times. [54] propose an SSI nowcasting model, SunCast, that predicts across North America based on GOES imagery and a ConvLSTM architecture with hourly updated forecasts and lead times of up to three hours. Similarly to [40], SunCast leverages a ConvLSTM architecture to simultaneously capture spatial and temporal dependencies. [40] train a six-layer autoencoder with three layers of encoder and decoder each and cloud index as the target variable, while [54] propose three stacked ConvLSTM layers. Both studies also include month and hour of the day as input features. While the SSI model of [40] relies on patch-based cropping of images, [54] process entire images. [55] combine a two-layer ConvLSTM with a four-layer Fourier neural operator (FNO) architecture trained with structural similarity loss to forecast SSI from Himawari satellite observations at 0.05° resolution. FNOs are neural networks that learn mappings between function spaces rather than finite-dimensional vector spaces. FNOs perform spectral convolutions that capture long-range spatial dependencies which makes them well suited for modelling cloud field motion over large domains [45]. [55] evaluate their model in a Chinese desert region (104–110°E, 35°–40°N). The model forecasts SSI at 10-minute intervals for lead times of up to one hour. As a benchmark, they compare it to ERA5 [56] which, due to its coarse resolution of more than 31 km, may be seen as a relatively lenient benchmark as spatial resolution is a major determining factor of SSI forecast accuracy.

3.2. Encoder–decoder convolutional networks

[42] present a spatiotemporal SSI forecast model that relies on visible GOES imagery input. Training different U-Net versions, [42]

find that a U-Net model that predicts differences between successive images rather than absolute future images performs the best at their SSI forecasting task. For a study area in southeastern South America, they demonstrate that their U-Net forecasts outperform IrradianceNet [40] and CMV-based forecasting approaches. Trained on MAE loss, their model yields SSI forecasts that gradually lose spatial detail as lead time increases. They also find that, compared to IrradianceNet, their U-Net model requires less training and inference time and can handle larger images. [43] present a U-Net model, HelioNet, to forecast cloud motion, following the U-Net architecture proposed by [48]. They first apply a Heliosat satellite retrieval to estimate cloud index fields from Meteosat imagery. Next, the U-Net model is used to forecast the derived cloud index fields, and subsequently the forecasts are converted to SSI fields. [43] benchmark the U-Net based forecasts to a cloud motion vector approach and find that the U-Net model improves over the CMV-based forecasts, particularly in winter months after 11 a.m. local time. They also report that, at the same time, the forecast model performs particularly poorly when night-time cloud index fields are input, including around sunrise. [57] train a U-Net with residual blocks and an integrated ConvLSTM to forecast SSI over northern China for forecast lead times of up to six hours. As U-Net models are not designed to inherently capture temporal processes, they insert the ConvLSTM between the U-Net's encoding and decoding layers with the goal to improve the model's forecast skill. For training, they utilise ERA5 and an SSI dataset that was derived from imagery of the geostationary FengYun satellite at 1.25 km spatial resolution and hourly sampling. They find that their SSI forecast model outperforms simple U-Net based predictions at all considered lead times.

3.3. Generative networks

Generative models have found widespread applications across many fields in recent years. Deep generative architectures relevant for solar forecasting include generative adversarial networks and diffusion models. Generative solar forecast models learn a conditional probability distribution $P(X_{\text{future}} \mid X_{\text{past}})$, which enables them to simulate multiple possible futures given the observed past. Generative models do not learn mappings like discriminative models but probability distributions, so they can generate arbitrary many new samples of plausible future SSI fields from the learned distribution. [45] present a generative diffusion model for probabilistic spatiotemporal SSI forecasting, SHADECast. They forecast clear-sky index fields derived from Meteosat, and train and test their model across central Europe. The model architecture comprises a variational autoencoder for compression to a latent space, a deterministic nowcaster that relies on adaptive FNO, a denoiser constituting the diffusion model, and a decompression step. Large-scale cloud evolution is predicted by the nowcaster in the latent space, whereas smaller-scale structure is generated by the diffusion model through successive denoising steps. SHADECast extends the forecast horizon by 26 min compared to the state-of-the-art statistical probabilistic forecast model SolarSTEPS [8], and outperforms bias-corrected forecasts from the highest-resolution configuration of the Integrated Forecasting System, IFS HRES, at lead times of up to approximately two hours [58]. The IFS HRES model operated by the European Centre for Medium-Range Weather Forecasts (ECMWF) is often used for SSI forecasting at intraday and day-ahead horizons [59,60]. SHADECast also provides significantly improved performance in predicting extreme values compared to the deterministic benchmark IrradianceNet. [44] utilise a conditional generative adversarial network (cGAN), DGMR-SO, to forecast SSI based on CSI predictions for lead times of up to four hours. Being an adversarial network, the model is based on adversarial training between a generator producing future SSI fields and discriminators. A spatial and a temporal discriminator are used that are trained to differentiate generated images from ground truth. The spatial discriminator relies on multiple two-dimensional CNNs for extracting spatial features whereas the temporal discriminator utilises three-dimensional CNNs to account for the time dimension. The model is benchmarked with a U-Net, an optical flow model and the numerical weather prediction model HARMONIE across the Netherlands. [44] find that the U-Net achieves the lowest forecast errors at most lead times as it utilises pixelwise loss functions that penalise deviations from mean future evolution, resulting in forecasts lacking sharpness, whereas DGMR-SO yields more realistic spatial patterns of its SSI forecasts and enables forecast ensemble generation. To our knowledge, SHADECast and DGMR-SO are the first probabilistic SSI forecast models based on next-frame prediction of satellite imagery. A major difference between them lies in the generative approach pursued by both studies. [45] achieve sharpness through successive diffusion steps, whereas [44] can maintain spatial detail through adversarial loss based training.

3.4. Transformers

Transformers are neural network architectures that utilise self-attention to model relationships within a sequence by weighting the relative importance of each element with respect to all others [68]. Transformers accept a sequence of tokens as input to predict the next item in the sequence. Given the sequence of tokens, a transformer captures their relationships and maps input tokens to contextual representations, enabling the prediction of subsequent sequence elements. [62] present a spatiotemporal transformer model for SSI forecasting, SolarFormer, that relies on the EarthFormer model [69] to estimate cloud motion. SolarFormer combines a transformer and a gated recurrent unit (GRU) model to estimate SSI from satellite. Forecasts are generated based on the previous two hours of observations for up to three hours ahead at 5 km horizontal resolution and 15-minute intervals. The GOES satellite data used to train and test the model are composed of 600 km × 600 km tiles around seven surface radiation budget observing network (SURFRAD) stations in the continental United States. Testing their model, [62] report that the accuracy of SolarFormer surpasses that of the High-Resolution Rapid Refresh (HRRR) model of the National Oceanic and Atmospheric Administration (NOAA) and that it achieves a lower relative RMSE and a lower relative bias than a ConvLSTM benchmark model.

3.5. Model intercomparison

While comparing the discussed network architectures and their performance for SSI forecasting lies beyond the scope of this review, we provide a general qualitative discussion of how the four model classes compare across aspects of next-frame prediction based on the findings of the reviewed studies (Table 1) and on surveys of next-frame prediction [46,70,71]. Spatiotemporal RNNs such as ConvLSTMs are inherently recurrent, which allows them to generate frames sequentially where each generated prediction is fed back into the model to generate the next prediction (roll-out). RNNs are suited to perform forecast roll-outs for any number of forecast steps without being restricted to fixed forecast horizons [40,43]. Spatiotemporal recurrent models can be suitable for resource-constrained hardware and edge deployment due to their moderate memory requirements [71]. They tend to be more data-efficient than transformers for learning moderately complex spatiotemporal dynamics, so they usually require less comprehensive training datasets [43]. Encoder–decoder CNN architectures such as U-Nets enable comparably short inference times [42]. Like spatiotemporal recurrent networks, this makes them suitable for resource-constrained hardware and for SSI forecast applications in which a short latency time is more important than realistically looking forecasts or forecast uncertainty quantification [71]. Encoder–decoder CNNs are often trained in a non-autoregressive manner to predict multiple future SSI fields in a single forward pass, thereby reducing error accumulation from multiple roll-out steps [42,43,71]. Encoder–decoder CNNs tend to be less complex to train than generative models, usually relying on standard MSE or MAE losses that minimise mean pixel differences [42,

Table 1
Satellite-based SSI forecast models based on next-frame prediction, in descending order by year of publication. The *Uncert.* column indicates deterministic (Det.) versus probabilistic (Prob.) models. The *Step* and *Hor.* columns indicate the time step of the training data and the maximum forecast lead time (forecast horizon) considered in the respective study. The *Type* column indicates generative (Gen.) versus discriminative (Disc.) models.

Ref.	Architecture	Satellite	Training data	Region	Step	Hor.	Uncert.	Type
[57]	U-Net	FengYun	HelioFY2 [61]	China	1 h	6 h	Det.	Disc.
[62]	Transformer	GOES	Channels	U.S.A.	15 min	3 h	Det.	Disc.
[55]	ConvLSTM	Himawari	Channels	China	10 min	1 h	Det.	Disc.
[45]	Diffusion	MSG	HelioMont [63,64]	Europe	15 min	2 h	Prob.	Gen.
[44]	cGAN	MSG	CPP [53,65]	Europe	15 min	4 h	Prob.	Gen.
[43]	U-Net	MSG	CI [66]	Europe	15 min	4 h	Det.	Disc.
[42]	U-Net	GOES	Albedo	South America	10 min	5 h	Det.	Disc.
[54]	ConvLSTM	GOES	SSI	North America	1 h	3 h	Det.	Disc.
[41]	ConvGRU	MSG	CPP [53]	Europe	15 min	6 h	Det.	Disc.
[40]	ConvLSTM	MSG	SARAH-2.1 [52]	Europe	30 min	4 h	Det.	Disc.
[51]	ConvLSTM	COMS	SSI [67]	South Korea	1 h	1 h	Det.	Disc.

44], but suffer from blurriness growing with increasing forecast lead times [44,45]. Encoder–decoder CNNs and convolutional RNNs rely on local convolutional kernels rather than global mechanisms such as attention or graph structures. Generative models enable realistically looking SSI forecasts. They are also well suited for ensemble simulations and forecast uncertainty quantification. Compared to other model architectures, generative models tend to suffer from longer inference times as they require potentially large numbers of denoising steps [45,71], typically predicting fewer frames per second than other networks for the same prediction task [44,45,71]. Generative models can be more complex to train than RNNs and encoder–decoder CNNs. They can suffer from unstable training and mode collapse, with the potential to produce only limited outputs and ignore the diversity of the underlying training data [44,70]. Transformers are well suited to model complex non-local long-range dependencies, unlike CNNs which enable only a local focus [62,70]. Transformers may hold the potential to extend prediction to longer lead times, opening opportunities for future research, while at the same time requiring increased training time and memory resources [62,71].

4. Probabilistic spatiotemporal SSI nowcasting

Most satellite-based spatiotemporal SSI nowcast models are deterministic (Table 1), providing point estimates of SSI at each pixel and therefore lacking the capability to quantify forecast uncertainty. Deterministic models tend to provide blurry SSI forecasts as they typically minimise an error-based loss function – usually the MSE or MAE – that favours forecasts close to the mean of the future SSI distribution and penalises deviations from it. Consequently, deterministic SSI forecasts typically do not feature sufficient spatiotemporal variability in the surface solar irradiance fields and exhibit blurriness that is growing with forecast lead time. As deterministic model forecasts tend to converge towards future mean SSI values, they usually also struggle with capturing extreme SSI intensities.

Probabilistic SSI forecasts predict probability distributions of future SSI fields [72]. Two probabilistic models for intraday spatiotemporal SSI forecasting have been proposed to date (Table 1), SHADECast and DGMR-SO [44,45]. Fig. 2 illustrates how SSI ensemble forecasts can be leveraged for probabilistic PV production forecasts. Due to their sampling from a probability distribution, both models maintain sharp spatial structures with progressing lead times and can simulate non-stationary CSI, such as overcast conditions that are clearing rapidly. SHADECast is a generative diffusion model while DGMR-SO is a generative adversarial network (Section 3.3). Both generative SSI forecasting methods model the distribution of possible future SSI fields across large spatial domains and sample from the estimated distribution to generate ensembles of SSI field forecasts. In addition to DGMR-SO and SHADECast, [40] proposed an adaptation to their deterministic SSI forecast model IrradianceNet to render it probabilistic by predicting, for every pixel, the probability that the clear-sky index falls within a specific interval. However, this classification approach inflates the output size by more than two orders of magnitude, rendering it impractical for large domains and forecasts over multiple lead times.

The choice between deterministic and probabilistic SSI forecast approaches involves trade-offs with regard to uncertainty quantification, computational cost, and further considerations. Deterministic models, such as ConvLSTMs and U-Nets, estimate a one-to-one mapping from previous SSI fields to a single future SSI field at each lead time. They typically minimise an MSE or MAE loss function to this end. Probabilistic SSI forecast models like GANs and diffusion models learn a conditional probability distribution, based on which an arbitrary number of realistically looking future SSI fields can be sampled. While deterministic models tend to be faster to train and have shorter inference times, they only provide one future realisation for each lead time, limiting their capabilities for uncertainty quantification and their usefulness in probabilistic future scenarios. Deterministic models usually struggle to predict extreme SSI values as they tend to forecast the conditional mean of the SSI field distribution at different lead times, providing blurry forecasts without high-resolution structural details. In contrast, probabilistic models can generate realistically looking future SSI fields by sampling from the learnt conditional probability distribution. This enables uncertainty quantification based on the predicted SSI field ensemble forecast. Generative probabilistic models predict sharp SSI fields and provide improved extreme value prediction. They can also model temporal distributional changes — such as transitions to more overcast or clearer conditions — that stationary deterministic models struggle to capture [45]. On the other hand, generative probabilistic models tend to suffer from higher computational cost and potentially worse training stability. Although visually more realistic, individual ensemble members can exhibit higher pixel-wise errors than deterministic models, as they favour physically plausible SSI fields over regression towards the conditional mean.

5. Validation and deployment of SSI forecast models

5.1. Validation of SSI forecast models

Validating spatiotemporal SSI forecast models involves assessing how well the predicted fields represent the actual future evolution of SSI. To characterise their quality, SSI forecasts can be compared with future SSI fields or future ground-based SSI observations based on metrics that quantify the accuracy, bias, and ensemble-based characteristics such as the reliability and sharpness of the forecasts. Forecast validation further includes analysing any systematic spatiotemporal patterns in forecast errors and biases, and examining how forecast quality depends on lead time, geographic region, solar zenith angle, and other conditions. Deterministic SSI forecasts predict a single SSI field at a given lead time. Their validation usually focuses on pointwise

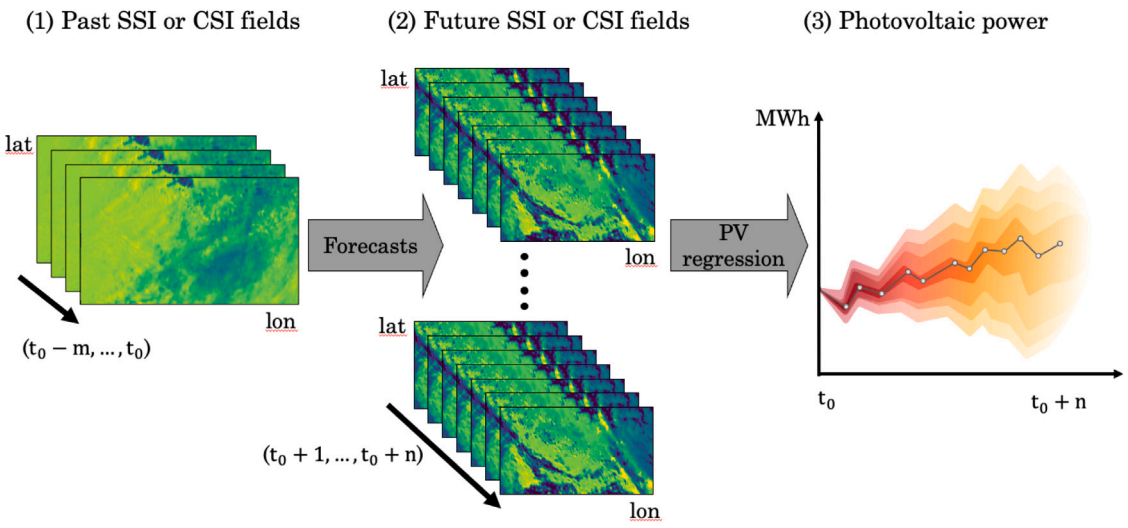

Fig. 2. Probabilistic spatiotemporal forecasting of SSI based on geostationary satellites enables probabilistic forecasts of PV production across large spatial domains.

accuracy and bias, usually quantified using metrics such as the root mean square error (RMSE) and MAE, while mean bias error (MBE) is used to assess systematic over- or underestimation. Forecast skill is often expressed relative to benchmark models, such as persistence, smart persistence, optical flow models, or numerical weather prediction models, using suitable skill scores. Probabilistic SSI forecasts, also referred to as ensemble forecasts, provide a set of plausible future SSI fields and thereby enable explicit representation of forecast uncertainty. Validating a probabilistic forecast model should include an assessment of how well the model captures forecast uncertainty. In probabilistic forecast validation, the forecast reliability is usually evaluated first. Forecast reliability is typically assessed using rank histograms, which are a diagnostic tool to qualitatively assess the forecast calibration. Rank histograms indicate how frequently observed SSI forecasts fall within the SSI forecast ensemble members after those members have been sorted by their rank [73]. A flat rank histogram indicates a well-calibrated ensemble, while systematic deviations from a flat rank histogram point to forecast model deficiencies. For example, in underdispersed forecasts, the spread of the SSI forecast ensemble is too narrow compared to observed SSI, meaning that SSI observations tend to fall outside the ensemble range, causing a U-shaped rank histogram.

Once the forecast reliability has been established, forecast sharpness and overall forecast skill are assessed. The forecast method's reliability is ensured first, and the forecast sharpness and overall performance are commonly evaluated after the reliability of the forecast method has been established. The idea is to maximise the forecast sharpness subject to the forecast reliability, avoiding sharp but unreliable forecasts (overconfidence). The continuous ranked probability score (CRPS) is among the most commonly used performance metrics in probabilistic forecast validation. It quantifies the overall forecast skill and implicitly accounts for both forecast reliability and sharpness. The CRPS generalises the MAE to probabilistic models and evaluates ensemble forecasts across the full probability distribution of predicted future SSI based on the distance between the forecast and the empirical cumulative distribution function [74,75].

Comprehensive evaluation and intercomparison of spatiotemporal SSI forecast models should go beyond aggregate performance metrics. In addition to analysing the spatial and temporal structure of forecast errors, their dependence on atmospheric and other conditions, and possible causes, forecast models should also be assessed with respect to their ability to generate sharp spatial structures, for example through visual inspection or by analysing power spectral densities to quantify how well the forecast SSI fields represent different spatial scales. Forecasts should ideally also be analysed in terms of their ability under specific weather conditions such as ramp events, convective cloud formation, and fog. Forecasts can be validated at the level of individual pixels and time steps, or using spatially or temporally aggregated quantities, such as regional or hourly-mean SSI forecasts. Reference data for SSI forecast validation include satellite-derived data products such as the Surface Radiation Dataset – Heliosat version 3 (SARAH-3) [76], reanalysis data such as ERA5, and ground-based measurements from pyranometers and sky cameras for local-scale forecast validation.

5.2. Operational deployment

The operational deployment of satellite-based SSI forecast models requires addressing several practical challenges going beyond model development. They relate to data availability at low latency, computational efficiency, spatial scalability, and the integration into energy system management and decision making, amongst others. A critical requirement is the timely and reliable acquisition of the relevant satellite data. Operational systems depend on near-real-time satellite imagery which typically becomes available every 10–15 min. SSI forecasts must be generated rapidly enough to remain useful for applications such as grid management and energy trading. This requires efficient data processing pipelines and fast model inference to run automatically, with minimal latency and update periods of 10–15 min in synchronisation with the satellite update cycles. It also requires robustness and fault tolerance. Satellite data streams can occasionally deliver corrupted images or contain missing images, for example due to sensor or calibration issues or temporary outages. Operationally deployed SSI forecast systems must be able to account for such conditions, for example, by means of persistence forecasts or other fallback models in case current satellite data is not available. To cover large areas, models can use a patch-based approach to handle large satellite image datasets. Patch-based forecasts tend to cause discontinuities at the patch boundaries. Scaling to larger regions may involve discarding the patch boundaries or, alternatively, developing a single model for the entire domain.

Operationally deployed SSI forecast models will benefit from continuous monitoring and improvement. The model forecast skill should be continuously monitored to identify any potential trends, variability and sources for improvement, which can lead to the development of even more skilful SSI forecast models. Finally, operational SSI forecasts can be integrated into downstream systems for energy-related applications such as grid balancing and energy trading. This can happen, for example, via application programming interfaces (APIs) that provide the SSI forecasts as a service to customer machines or via websites providing forecasts and suitable visualisations.

6. Research needs and future directions

Satellite-based SSI forecasting using deep learning offers strong potential for accurate spatiotemporal prediction of solar photovoltaic power production. Geostationary satellites provide wide-area coverage with high spatial resolution and minute-scale update frequencies, enabling low-latency initialisation of SSI forecasts from regional to global scales. Advanced neural networks applied to satellite observations allow simultaneous forecasting for large numbers of sites and entire PV fleets across grid zones, countries, and continents. Long-term satellite archives support the training of deep spatiotemporal models that treat SSI forecasting as a next-frame prediction problem. As demonstrated by recent studies, such models can outperform cloud-motion-vector-based approaches and conventional weather prediction at lead times of up to several hours, making satellite-based forecasts of SSI fields particularly attractive for applications in power production, grid operation, and energy trading. Many characteristics of the reviewed satellite-based SSI forecast models remain largely unexplored to date. For example, further research is needed to systematically investigate the conditions under which each model is preferable for SSI forecasting applications, considering spatial scale, meteorological conditions including cloud dynamics, data availability, and additional factors. In this section, we are discussing opportunities and challenges, and are outlining research needs and possible future research directions.

6.1. Fast shifts in cloudiness conditions and extremes

How spatiotemporal satellite-based SSI forecast models perform under conditions of rapidly changing cloudiness has received limited attention to date. Future studies should investigate SSI forecasting during periods of systematic brightening or darkening driven by rapid cloud cover changes over the course of up to several hours and during ramp events. In such conditions, the distribution of CSI values across the region of interest shifts systematically towards significantly higher or lower CSI values. Classical autoregressive models typically simulate stationary CSI distributions and therefore cannot capture shifts, whereas generative models are, in principle, able to simulate rapid changes in CSI distributions [8]. Beyond changing mean conditions, future research should also characterise satellite-based SSI forecast models with respect to their ability to represent extreme CSI values. Models trained to minimise error-based loss functions simulate forecasts that converge towards conditional mean SSI fields, which leads to an underrepresentation of extremes. Generative models, by contrast, can produce sharp realisations of future SSI fields and hold the potential to simulate extremes [44,45]. Future research should explore further approaches to maintain forecast sharpness and improve the representation of extremes, including the use of distributional loss functions such as CRPS-based losses and alternative network architectures to preserve spatial structure over time.

6.2. Uncertainty-aware forecasts

Deterministic forecast models such as ConvLSTMs do not intrinsically capture the uncertainty of a forecast, as they do not model the distribution of possible future SSI fields but predict a single SSI field at a given lead time. Probabilistic models can represent forecast uncertainty, which can be critical for decision making in electricity grid management and other fields. The predictability of SSI can vary substantially depending on the initial conditions. Only two satellite-based SSI forecast models have been presented to date that are capable of simulating ensembles of plausible future SSI fields and thereby representing forecast uncertainty, SHADECast and DGMR-SO [44,45]. Further approaches and architectures should be explored to improve probabilistic forecasts and their calibration, avoiding underdispersion. SSI field forecasts with a given probability should occur with that frequency in practice, avoiding systematic under- or overestimation of extremes and yielding approximately flat rank histograms during model validation.

6.3. Improving initial conditions

Accurate SSI forecasts critically depend on the quality of the initial conditions, making reliable SSI field estimates at initialisation time essential. Estimating SSI from satellite radiometers requires capturing atmospheric radiative transfer processes as well as land surface radiative properties and their temporal variability. Retrieval algorithms must also account for geometric effects, for example, in relation to viewing angles, cloud shadows, and apparent displacements of clouds arising from uncertainties in cloud top height estimates (parallax effect). Such displacement errors can introduce substantial SSI errors even at short lead times. By learning spatiotemporal context, machine-learning-based SSI retrievals have the potential to mitigate such errors. SSI retrieval algorithms can also struggle to distinguish clouds and aerosols from variable land cover and surface albedos, for example when differentiating snow-covered surfaces from cloud reflectances [64]. Radiative transfer modelling in complex environments, such as mountain regions, poses additional challenges [77]. Addressing these limitations is important, as uncertainties and biases in SSI retrievals can directly propagate into forecast initial conditions and subsequently degrade forecast skill. Further research is also needed to examine the role of sub-pixel variability, such as from fields of small cumulus clouds, cloud edges, and fine-scale aerosol plumes. While such conditions may be challenging to represent in satellite-based SSI retrievals, their radiative effects are implicitly captured by satellite radiometers. Understanding how unresolved sub-grid features influence SSI and how their impacts can be better represented in retrieval models remains a relevant research challenge. SSI forecasting at low solar elevation angles — particularly during early morning hours — is also challenging as early-morning forecasts are initialised with night-time satellite imagery [43,62]. Further research should therefore examine how infrared channels can be optimally combined with visible channels to improve forecasts in the early morning hours. Validating and characterising satellite-retrieved SSI estimates used for forecast model training is of critical importance. Systematic biases and overly large uncertainties in SSI retrieval products can propagate into SSI forecasts if not corrected. Even in the absence of biases, excessive uncertainty in the retrieved SSI fields introduces noise in training datasets, reducing the accuracy of the resulting forecasts. Deep networks can support bias correction and uncertainty reduction, for example by fine-tuning on high-quality ground-based pyranometer observations [30].

6.4. Leveraging and combining new data sources

Current satellite-based SSI forecast models typically rely on multi-annual observational records from a single geostationary satellite (Table 1). Further research should investigate the integration of additional observational data sources, and more generally the combination of multiple data sources, including ground-based sensors and weather prediction models, sometimes referred to as multi-source data fusion. New generations of Earth observing satellites, such as Meteosat Third Generation [78], provide enhanced capabilities, including additional spectral channels, shorter imaging repeat cycles, and higher spatial resolution. Leveraging new data sources may also involve combining satellite observations with additional ground-based measurements. Ground-based imaging and remote sensing systems can provide more detailed information on cloud conditions from local to regional scales. While pyranometer networks are sparse and offer limited spatial representativeness, they can provide highly accurate high-frequency SSI measurements that are valuable for model training and validation. Combining multiple sensor systems may also help improve the estimation of the ground radiative effect of differing cloud phases, optical properties, horizontal and vertical cloud structures. Incorporating aerosol information in satellite-based spatiotemporal SSI forecast models can further improve forecast quality. Despite their coarser resolution, reanalysis

data can be useful as additional sources for model training and validation, including the forthcoming sixth generation of the ECMWF atmospheric reanalysis of global weather and climate, ERA6.

Future studies may also explore incorporating PV production data as indirect estimates of SSI [79] for forecast applications. Further research should also investigate the representativeness of ground-based SSI measurements of their surroundings when comparing point-like pyranometer observations to satellite pixels of typically multiple km^2. Deep networks offer large potential to coherently combine and leverage heterogeneous data sources at differing resolutions, update frequencies, latency times, spatial representativeness, and measurement uncertainties. They can also serve to identify the most relevant data sources for skilful SSI forecasts. It can be challenging to utilise PV production data and other ground-based SSI-related datasets because of privacy concerns by the operators of PV sites or privately operated pyranometers. Future studies may investigate the potential of federated learning to utilise distributed data sources in a privacy-preserving manner without gaining access to the data itself [80]. First studies started to explore the application of federated learning algorithms for SSI forecasting on ground-based distributed data sources [81,82] but they remain limited to site-specific forecasts without exploring connections with satellite observations and predictions of dense SSI fields.

6.5. Generalisation and robustness

Models for estimating and forecasting SSI fields from satellite observations are usually developed and validated across specific regions with characteristic climate regimes and surface characteristics. As a result, models may implicitly learn region-specific relationships and exhibit reduced performance when applied outside their original domain. Limited diversity in training data can lead to biases and diminished forecast skill in regions with different climate regimes or surface properties, as model performance is strongly influenced by the range of atmospheric and surface conditions represented in the training data. Models trained under predominantly sunny conditions may exhibit reduced skill when applied to persistently cloudy regions, and when models developed over low-albedo surfaces are applied across high-albedo environments such as snow-, ice-, or sand-covered terrain. Seasonal variations in surface characteristics can further complicate model transferability. Evaluating the robustness and generalisability of SSI models across regions, climates, surface albedos, time of day, and seasons is therefore essential for both physics-based and deep-learning approaches [30,83]. Such assessments also depend on high-quality multi-annual SSI observations from ground-based pyranometers, which remain spatially sparse, especially in the Southern Hemisphere. Future work should investigate strategies to improve model transferability across different regions and the potential of transfer learning approaches.

6.6. Benchmarking and comparability

More comprehensive intercomparisons of satellite-based SSI forecast models based on next-frame prediction will be beneficial. Various models have been proposed (Table 1) but performance comparisons among them are hardly possible currently because the models have been trained on different regions with different climates and weather conditions. The regions also differ in terms of land cover types and associated surface albedos. Different training and test periods were used, with observations from different satellite platforms and ground sensor systems, different SSI data products and computing environments in which the models were trained and forecasts were run. Further differences relate to the preprocessing of input data and the forecast task definition including the lead times and forecast intervals. Differences also arise from the chosen training, validation and test strategies, for example, from temporal and spatial sampling and aggregation, training-validation-test splits, training parameters, evaluation metrics, site-specific or full-field evaluation, and the postprocessing of the SSI forecasts, including bias correction and site-specific finetuning. Most reviewed studies do not release the exact datasets used for training and evaluation, and only a few provide trained models or code [40,44,45]. A comparison among the models would require redeveloping models based on the related publications, which may come with uncertainties due to potentially incomplete methodological descriptions in view of the various choices and steps involved in SSI forecast model development. To achieve comparability, all models would need to be trained and tested on the same training and test sets. Establishing a common benchmark dataset and protocol for satellite-based spatiotemporal SSI forecasting would facilitate intercomparisons of existing and future models. While potential benchmark datasets exist (e.g., [84]), community adoption towards common benchmarks and datasets has yet to emerge. Unlike other machine learning domains, the absence of common benchmarks in SSI forecasting likely also reflects the strong regional focus of many studies, which are often concentrated on the geographic areas of interest of the contributing institutions.

6.7. Integration of data-driven learning and physical modelling

Combining data-driven and physical modelling for energy forecasts may have the potential to advance SSI forecast models. Such hybrid models commonly combine physical laws and machine learning. This can involve, for example, physical modelling of radiative transfer and equations of motions, combined with machine learning on observational datasets. Physical models tend to provide physically consistent estimates and are in principle able to simulate extreme events. Machine learning models can learn representations of highly non-linear processes but may also learn systematic errors present in training data and can struggle to extrapolate to extremes. Hybrid models can involve the design of physically inspired neural network architectures that reflect the physical processes to be modelled [45,85,86]; the incorporation of physical laws or constraints as regularisation terms in the loss function [87,88]; the use of machine-learning-based parameterisations within physics-based SSI forecast or retrieval models; and the application of machine learning for bias correction or, more generally, postprocessing of physics-based forecasts [89]. One promising example arises from the complementary strengths of physical and data-driven approaches in satellite-based SSI retrievals. For a given atmospheric composition, clear-sky SSI can be computed with high accuracy, as it primarily depends on solar geometry which is determined by location and time via the solar zenith angle. In contrast, machine learning based SSI retrievals tend to perform better at retrieving SSI from satellites in cloudy or overcast conditions but show scope for improvment under clear-sky conditions [30,83]. Future research should explore SSI forecasting approaches that combine physics-based clear-sky SSI estimates with machine learning based CSI or SSI estimates in cloudy conditions. A further example concerns cloud motion, which can be conceptualised as a combination of large-scale advection and smaller-scale, stochastic cloud evolution driven by processes such as turbulence. Further exploration of hybrid modelling approaches that combine data-driven learning and physical modelling can hold potential for improving satellite-based SSI forecasting.

6.8. Computational cost and operational deployment

Satellite-based SSI forecast model development faces several practical challenges related to required data volume, image sizes, and training cost, especially when models are developed for large spatial domains. Geostationary satellites provide imagery every 10–15 min, and multi-annual archives can contain hundreds of thousands of images. When each image covers large regions at kilometer-scale resolution and potentially in multiple channels, storage and data-loading can become bottlenecks. Efficient preprocessing and data pipelines are required to reduce overall model training time. Forecast skill can benefit from larger spatial context since cloud systems can evolve over hundreds

of kilometers. High-resolution full-disk or regional satellite images can make processing and model training memory-intensive. Some models like IrradianceNet address this by splitting images into patches, which reduces memory usage but may introduce boundary artefacts and lose long-range spatial dependencies. Long training times may be involved. Spatiotemporal models must process sequences of large images, which tends to increase GPU memory requirements and computation time. Training on multi-annual datasets can take days to weeks, depending on the available GPU infrastructure, which tends to limit the exploration of different architectures and hyperparameters. The reviewed studies handle such constraints differently, which can further complicate the benchmarking and reproducibility across SSI forecast models. Operational deployment of SSI forecast models requires rapid and frequent inference. Compared with physical models, deep neural networks can achieve significantly shorter runtimes, allowing near-instantaneous SSI retrieval and forecasts at regional to continental scales, in principle only limited by the satellite's scan frequency. Nevertheless, deep neural networks such as generative models can still take time to converge in training and run forecasts with. Strategies that were presented for speed up include staged training to forecast only the next time step and transfer learning by initialising with the weights of a pretrained model, e.g. [43,44]. Future work should investigate additional methods to improve training efficiency and shorten inference time to further reduce the computational demands of developing and running SSI forecast models based on next-frame prediction.

6.9. Modelling large-scale PV production

For SSI forecasts to be operationally useful in energy system applications, predicted SSI fields must be translated into solar PV power production. Mapping SSI to PV production and evaluating solar forecast models in terms of their skill in predicting PV production requires information on the installed operational capacity and ideally multi-annual production time series from large numbers of distributed PV systems. Previous studies on SSI field and PV forecasting rely on small sets of PV stations, e.g. [55]. Even studies on ground-based SSI forecasting usually do no involve more than a few dozen PV systems [90–92] and used at most 316 stations for training and validation of SSI forecast models [86]. However, [58] recently introduced the first large-scale validation using a dense fleet of more than 6400 distributed PV systems, enabling detailed analysis and visualisation of the radiative impacts of cloud systems on the national PV power generation. Future research should extend SSI and PV forecasting to large representative PV fleets as relevant in power generation, grid balancing, in combination with wind energy and demand forecasting, and for decision making in energy systems and markets.

Declaration of competing interest

The authors declare that they have no known competing financial interests or personal relationships that could have appeared to influence the work reported in this paper.

Acknowledgements

We thank the anonymous reviewers for their comments which helped to improve the manuscript. Funding by the Swiss National Science Foundation, Switzerland (grant number 200654) is acknowledged for aspects of this project.

Data availability

No data was used for the research described in the article.

References

[1] International Energy Agency. Renewables 2025. 2025, URL: https://www.iea.org/reports/renewables-2025.
[2] Goodarzi S, Niles Perera H, Bunn D. The impact of renewable energy forecast errors on imbalance volumes and electricity spot prices. Energy Policy 2019. http://dx.doi.org/10.1016/j.enpol.2019.06.035.
[3] Visser L, et al. Probabilistic solar power forecasting: An economic and technical evaluation of an optimal market bidding strategy. Appl Energy 2024. http://dx.doi.org/10.1016/j.apenergy.2024.123573.
[4] Kaur A, et al. Benefits of solar forecasting for energy imbalance markets. Renew Energy 2016. http://dx.doi.org/10.1016/j.renene.2015.09.011.
[5] Gueymard C, Myers D. Solar radiation measurement: Progress in radiometry for improved modeling. Model Sol Radiat Earth's Surf 2008. http://dx.doi.org/10.1007/978-3-540-77455-6_1.
[6] Wild M, et al. The global energy balance from a surface perspective. Clim Dyn 2013;40. http://dx.doi.org/10.1007/s00382-012-1569-8.
[7] Siebesma P, et al. Clouds and climate: Climate science's greatest challenge. Cambridge University Press; 2020, http://dx.doi.org/10.1017/9781107447738.
[8] Carpentieri A, et al. Intraday probabilistic forecasts of surface solar radiation with cloud scale-dependent autoregressive advection. Appl Energy 2023;351. http://dx.doi.org/10.1016/j.apenergy.2023.121775.
[9] Giorgetta M, et al. ICON-A, the atmospheric component of the ICON earth system model: I. model description. J Adv Model Earth Syst 2018;10. http://dx.doi.org/10.1029/2017MS001242.
[10] Bengtsson L, et al. The HARMONIE–AROME model configuration in the ALADIN–HIRLAM NWP system. Mon Weather Rev 2017;145. http://dx.doi.org/10.1175/MWR-D-16-0417.1.
[11] European Centre for Medium-Range Weather Forecasts. Dissemination schedule. 2025, URL: https://confluence.ecmwf.int/display/DAC/Dissemination+schedule.
[12] Sultana N, Tsutsumida N. A review on data-driven methods for solar energy forecasting. Appl Energy 2025;400. http://dx.doi.org/10.1016/j.apenergy.2025.126631.
[13] Yang D, et al. A review of solar forecasting, its dependence on atmospheric sciences and implications for grid integration: Towards carbon neutrality. Renew Sustain Energy Rev 2022;161. http://dx.doi.org/10.1016/j.rser.2022.112348.
[14] Ahmed R, et al. A review and evaluation of the state-of-the-art in PV solar power forecasting: Techniques and optimization. Renew Sustain Energy Rev 2020;124. http://dx.doi.org/10.1016/j.rser.2020.109792.
[15] Rodríguez-Benítez F, et al. Assessment of new solar radiation nowcasting methods based on sky-camera and satellite imagery. Appl Energy 2021;292. http://dx.doi.org/10.1016/j.apenergy.2021.116838.
[16] Vuilleumier L, et al. Accuracy of satellite-derived solar direct irradiance in Southern Spain and Switzerland. Int J Remote Sens 2020;41. http://dx.doi.org/10.1080/01431161.2020.1783712.
[17] Hammer A, et al. Short-term forecasting of solar radiation: a statistical approach using satellite data. Solar Energy 1999;67. http://dx.doi.org/10.1016/S0038-092X(00)00038-4.
[18] Arbizu-Barrena C, et al. Short-term solar radiation forecasting by advecting and diffusing MSG cloud index. Solar Energy 2017;155. http://dx.doi.org/10.1016/j.solener.2017.07.045.
[19] Ayet A, Tandeo P. Nowcasting solar irradiance using an analog method and geostationary satellite images. Solar Energy 2017;164. http://dx.doi.org/10.1016/j.solener.2018.02.068.
[20] Wen H, et al. A regional solar forecasting approach using generative adversarial networks with solar irradiance maps. Renew Energy 2023;216. http://dx.doi.org/10.1016/j.renene.2023.119043.
[21] Liao Z, Coimbra C. Hybrid solar irradiance nowcasting and forecasting with the scope method and convolutional neural networks. Renew Energy 2024;232. http://dx.doi.org/10.1016/j.renene.2024.121055.
[22] Chen S, et al. Improved satellite-based intra-day solar forecasting with a chain of deep learning models. Energy Convers Manage 2024;313. http://dx.doi.org/10.1016/j.enconman.2024.118598.
[23] Berthomier L, Pradel B, Perez L. Cloud cover nowcasting with deep learning. 2020, URL: https://arxiv.org/pdf/2009.11577.
[24] Xia P, et al. Accurate nowcasting of cloud cover at solar photovoltaic plants using geostationary satellite images. Nat Commun 2024;15. http://dx.doi.org/10.1038/s41467-023-44666-1.
[25] Tarpley J. Estimating incident solar radiation at the surface from geostationary satellite data. J Appl Meteorol Climatol 1979. http://dx.doi.org/10.1175/1520-0450(1979)018<1172:EISRAT>2.0.CO;2.
[26] Huang G, et al. Estimating surface solar irradiance from satellites: Past, present, and future perspectives. Remote Sens Environ 2019;233. http://dx.doi.org/10.1016/j.rse.2019.111371.
[27] Cano D, et al. A method for the determination of the global solar radiation from meteorological satellite data. Solar Energy 1986;37. http://dx.doi.org/10.1016/0038-092X(86)90104-0.
[28] Rigollier C, Lefèvre M, Wald L. The method heliosat-2 for deriving shortwave solar radiation from satellite images. Solar Energy 2004;77. http://dx.doi.org/10.1016/j.solener.2004.04.017.

[29] Ineichen P. A broadband simplified version of the Solis clear sky model. Solar Energy 2008;82. http://dx.doi.org/10.1016/j.solener.2008.02.009.

[30] Schuurman K, Meyer A. Surface solar radiation: AI satellite retrieval can outperform heliosat and generalizes to other climate zones. Int J Remote Sens 2025;46. http://dx.doi.org/10.1080/01431161.2025.2471596.

[31] Leese J, Novak C, Clark B. An automated technique for obtaining cloud motion from geosynchronous satellite data using cross correlation. J Appl Meteorol Climatol 1971;10. http://dx.doi.org/10.1175/1520-0450(1971)010<0118:AATFOC>2.0.CO;2.

[32] Wang P, et al. Surface solar radiation forecasts by advecting cloud physical properties derived from meteosat second generation observations. Solar Energy 2019;177. http://dx.doi.org/10.1016/j.solener.2018.10.073.

[33] Kleissl J, editor. Solar forecasting and resource assessment. 2013, http://dx.doi.org/10.1016/C2011-0-07022-9.

[34] Cros S, et al. Extracting cloud motion vectors from satellite images for solar power forecasting. In: 2014 IEEE geoscience and remote sensing symposium. 2014, http://dx.doi.org/10.1109/IGARSS.2014.6947394.

[35] Aicardi D, Musé P, Alonso-Suárez R. A comparison of satellite cloud motion vectors techniques to forecast intra-day hourly solar global horizontal irradiation. Solar Energy 2022;233. http://dx.doi.org/10.1016/j.solener.2021.12.066.

[36] Fortun D, Bouthemy P, Kervrann C. Optical flow modeling and computation: A survey. Comput Vis Image Underst 2015;134. http://dx.doi.org/10.1016/j.cviu.2015.02.008.

[37] Lucas B, Kanade T. An iterative image registration technique with an application to stereo vision. In: Proc 7th intl joint conf on artificial intelligence. IJCAI 1981, 1981, URL: https://www.ri.cmu.edu/pub_files/pub3/lucas_bruce_d_1981_1/lucas_bruce_d_1981_1.pdf.

[38] Zhai M, et al. Optical flow and scene flow estimation: A survey. Pattern Recognit 2020;114. http://dx.doi.org/10.1016/j.patcog.2021.107861.

[39] Marty C, Philipona R. The clear-sky index to separate clear-sky from cloudy-sky situations in climate research. Geophys Res Lett 2000;27. http://dx.doi.org/10.1029/2000GL011743.

[40] Nielsen A, Iosifidis A, Karstoft H. IrradianceNet: Spatiotemporal deep learning model for satellite-derived solar irradiance short-term forecasting. Solar Energy 2021;228. http://dx.doi.org/10.1016/j.solener.2021.09.073.

[41] Knol D, et al. Deep learning for solar irradiance nowcasting: A comparison of a recurrent neural network and two traditional methods. In: Computational science – ICCS 2021. vol. 12746, 2021, http://dx.doi.org/10.1007/978-3-030-77977-1_24.

[42] Marchesoni-Acland F, et al. Deep learning methods for intra-day cloudiness prediction using geostationary satellite images in a solar forecasting framework. Solar Energy 2023;262. http://dx.doi.org/10.1016/j.solener.2023.111820.

[43] Straub N, et al. Satellite-based solar irradiance forecasting: Replacing cloud motion vectors by deep learning. Solar RRL 2024;8. http://dx.doi.org/10.1002/solr.202400475.

[44] Cui Y, et al. Solar radiation nowcasting based on geostationary satellite images and deep learning models. Solar Energy 2024;282. http://dx.doi.org/10.1016/j.solener.2024.112866.

[45] Carpentieri A, et al. Extending intraday solar forecast horizons with deep generative models. Appl Energy 2024;377. http://dx.doi.org/10.1016/j.apenergy.2024.124186.

[46] Zhou Y, Dong H, El Saddik A. Deep learning in next-frame prediction: A benchmark review. IEEE Access 2020;8. http://dx.doi.org/10.1109/ACCESS.2020.2987281.

[47] Shi X, et al. Convolutional LSTM network: A machine learning approach for precipitation nowcasting. 2015, doi:https://arxiv.org/abs/1506.04214.

[48] Ronneberger O, Fischer P, Brox T. U-Net: Convolutional networks for biomedical image segmentation. 2015, doi:https://arxiv.org/abs/1505.04597.

[49] Creswell A, et al. Generative adversarial networks: An overview. IEEE Signal Process Mag 2018;35. http://dx.doi.org/10.1109/MSP.2017.2765202.

[50] Cao H, et al. A survey on generative diffusion models. IEEE Trans Knowl Data Eng 2024;36. http://dx.doi.org/10.1109/TKDE.2024.3361474.

[51] Yeom J, et al. Spatial mapping of short-term solar radiation prediction incorporating geostationary satellite images coupled with deep convolutional LSTM networks for South Korea. Environ Res Lett 2020;15. http://dx.doi.org/10.1088/1748-9326/ab9467.

[52] Pfeifroth U, et al. Trends and variability of surface solar radiation in europe based on surface- and satellite-based data records. J Geophys Res: Atmos 2018;123. http://dx.doi.org/10.1002/2017JD027418.

[53] Roebeling R, Feijt A, Stammes P. Cloud property retrievals for climate monitoring: Implications of differences between Spinning Enhanced Visible and Infrared Imager (SEVIRI) on METEOSAT-8 and Advanced Very High Resolution Radiometer (AVHRR) on NOAA-17. J Geophys Res: Atmos 2006;111. http://dx.doi.org/10.1029/2005JD006990.

[54] Kumaresan D, et al. SunCast: Solar irradiance nowcasting from geosynchronous satellite data. 2022, URL: https://arxiv.org/pdf/2201.06173.

[55] Wu H, et al. Machine learning forecasts of short wave radiation from geostationary satellite measurements to optimize solar photovoltaic and concentrated solar power systems. Solar Energy 2025;299. http://dx.doi.org/10.1016/j.solener.2025.113718.

[56] Hersbach H, et al. The ERA5 global reanalysis. Q J R Meteorol Soc 2020;146. http://dx.doi.org/10.1002/qj.3803.

[57] Ruan Z, et al. Spatiotemporal solar radiation forecasting driven by satellite-based and reanalysis data for distributed PV integration using fully-convolutional neural network. Renew Energy 2025;256. http://dx.doi.org/10.1016/j.renene.2025.124556.

[58] Lanzilao L, Meyer A. Intraday spatiotemporal PV power prediction at national scale using satellite-based solar forecast models. 2026, http://dx.doi.org/10.48550/arXiv.2601.04751.

[59] Yang D, et al. Verifying operational intra-day solar forecasts from ECMWF and NOAA. Solar Energy 2022;236. http://dx.doi.org/10.1016/j.solener.2022.03.004.

[60] Wang W, et al. An archived dataset from the ECMWF ensemble prediction system for probabilistic solar power forecasting. Solar Energy 2022;248. http://dx.doi.org/10.1016/j.solener.2022.10.062.

[61] Huang C, et al. Retrieval of sub-kilometer resolution solar irradiance from Fengyun-4A satellite using a region-adapted Heliosat-2 method. Solar Energy 2023;264. http://dx.doi.org/10.1016/j.solener.2023.112038.

[62] Li R, et al. Transformer approach to nowcasting solar energy using geostationary satellite data. Appl Energy 2025;377. http://dx.doi.org/10.1016/j.apenergy.2024.124387.

[63] Castelli M, et al. The HelioMont method for assessing solar irradiance over complex terrain: Validation and improvements. Remote Sens Environ 2014;152. http://dx.doi.org/10.1016/j.rse.2014.07.018.

[64] Carpentieri A, et al. Satellite-derived solar radiation for intra-hour and intra-day applications: Biases and uncertainties by season and altitude. Solar Energy 2023;255. http://dx.doi.org/10.1016/j.solener.2023.03.027.

[65] Benas N, et al. CLAAS-3: the third edition of the CM SAF cloud data record based on SEVIRI observations. Earth Syst Sci Data 2023;15. http://dx.doi.org/10.5194/essd-15-5153-2023.

[66] Hammer A, et al. Solar energy assessment using remote sensing technologies. Remote Sens Environ 2003;86. http://dx.doi.org/10.1016/S0034-4257(03)00083-X.

[67] Yeom J, Han K, Kim J. Evaluation on penetration rate of cloud for incoming solar radiation using geostationary satellite data. Asia-Pac J Atmos Sci 2012;48. http://dx.doi.org/10.1007/s13143-012-0011-9.

[68] Vaswani A, et al. Attention is all you need. 2017, doi:https://arxiv.org/abs/1706.03762.

[69] Gao Z, et al. Earthformer: Exploring space-time transformers for earth system forecasting. 2022, doi:https://arxiv.org/abs/2207.05833.

[70] Oprea S, et al. A review on deep learning techniques for video prediction. IEEE Trans Pattern Anal Mach Intell 2020;44. http://dx.doi.org/10.1109/TPAMI.2020.3045007.

[71] Chen Z, et al. Predictive autonomy for UAV remote sensing: A survey of video prediction. Remote Sens 2025;17. http://dx.doi.org/10.3390/rs17203423.

[72] Gneiting T, Katzfuss M. Probabilistic forecasting. Annu Rev Stat Appl 2014;1. http://dx.doi.org/10.1146/annurev-statistics-062713-085831.

[73] Hamill T. Interpretation of rank histograms for verifying ensemble forecasts. Mon Weather Rev 2001;129. http://dx.doi.org/10.1175/1520-0493(2001)129<0550:IORHFV>2.0.CO;2.

[74] Gneiting T, Raftery A. Strictly proper scoring rules, prediction, and estimation. J Stat Assoc 2007;102. http://dx.doi.org/10.1198/016214506000001437.

[75] Hersbach H. Decomposition of the continuous ranked probability score for ensemble prediction systems. Weather Forecast 2000;15. http://dx.doi.org/10.1175/1520-0434(2000)015<0559:DOTCRP>2.0.CO;2.

[76] Pfeifroth U, et al. SARAH-3 – satellite-based climate data records of surface solar radiation. Earth Syst Sci Data 2024;16. http://dx.doi.org/10.5194/essd-16-5243-2024.

[77] Chen Y, Hall A, Liou K. Application of three-dimensional solar radiative transfer to mountains. J Geophys Res: Atmos 2006;111. http://dx.doi.org/10.1029/2006JD007163.

[78] Holmlund K, et al. Meteosat third generation (MTG): Continuation and innovation of observations from geostationary orbit. Bull Am Meteorol Soc 2021;102. http://dx.doi.org/10.1175/BAMS-D-19-0304.1.

[79] Barry J, et al. Irradiance and cloud optical properties from solar photovoltaic systems. Atmos Meas Tech 2023;16. http://dx.doi.org/10.5194/amt-16-4975-2023.

[80] Grataloup A, Jonas S, Meyer A. A review of federated learning in renewable energy applications: Potential, challenges, and future directions. Energy AI 2024;17. http://dx.doi.org/10.1016/j.egyai.2024.100375.

[81] Wen H, et al. A solar forecasting framework based on federated learning and distributed computing. Build Environ 2022;225. http://dx.doi.org/10.1016/j.buildenv.2022.109556.

[82] Moradzadeh A, et al. A novel cyber-resilient solar power forecasting model based on secure federated deep learning and data visualization. Renew Energy 2023;211. http://dx.doi.org/10.1016/j.renene.2023.04.055.

[83] Verbois H, et al. Retrieval of surface solar irradiance from satellite imagery using machine learning: pitfalls and perspectives. Atmos Meas Tech 2023. http://dx.doi.org/10.5194/amt-16-4165-2023.

[84] Li R, et al. SolarCube: An integrative benchmark dataset harnessing satellite and in-situ observations for large-scale solar energy forecasting. In: Advances in neural information processing systems. NeurIPS 2024, 2024, http://dx.doi.org/10.52202/079017-0115.

[85] Yang Y, et al. DEST-GNN: A double-explored spatio-temporal graph neural network for multi-site intra-hour PV power forecasting. Appl Energy 2025;378. http://dx.doi.org/10.1016/j.apenergy.2024.124744.

[86] Karimi A, et al. Spatiotemporal graph neural network for performance prediction of photovoltaic power systems. Proc AAAI Conf Artif Intell 2021;35. http://dx.doi.org/10.1609/aaai.v35i17.17799.

[87] Kashinath K, et al. Physics-informed machine learning: case studies for weather and climate modelling. Philos Trans R Soc A 2021. http://dx.doi.org/10.1098/rsta.2020.0093.

[88] Raissi M, Perdikaris P, Karniadakis G. Physics-informed neural networks: A deep learning framework for solving forward and inverse problems involving nonlinear partial differential equations. J Comput Phys 2019;378. http://dx.doi.org/10.1016/j.jcp.2018.10.045.

[89] Verbois H, et al. Statistical learning for NWP post-processing: A benchmark for solar irradiance forecasting. Solar Energy 2022;238. http://dx.doi.org/10.1016/j.solener.2022.03.017.

[90] Ali M, et al. Enhancing PV power forecasting through feature selection and artificial neural networks: a case study. Sci Rep 2025;15. http://dx.doi.org/10.1038/s41598-025-07038-x.

[91] Diaz-Bello D, Vargas-Salgado C, Alcazar-Ortega M. Optimizing photovoltaic power plant forecasting with dynamic neural network structure refinement. Sci Re 2025;15. http://dx.doi.org/10.1038/s41598-024-80424-z.

[92] van der Meer D, Munkhammar J, Widen J. Probabilistic forecasting of solar power, electricity consumption and net load: Investigating the effect of seasons, aggregation and penetration on prediction intervals. Sol Energy 2018;171. http://dx.doi.org/10.1016/j.solener.2018.06.103.